ACCOUNTS of chemical research

pubs.acs.org/accounts Article

# Advancing Chelation Strategies for Large Metal Ions for Nuclear Medicine Applications

Aohan Hu and Justin J. Wilson*

Cite This: *Acc. Chem. Res.* 2022, 55, 904−915 Read Online

ACCESS | Metrics & More | Article Recommendations



**CONSPECTUS:** Nuclear medicine leverages radioisotopes of a wide range of elements, a significant portion of which are metals, for the diagnosis and treatment of disease. To optimally use radioisotopes of the metal ions, or radiometals, for these applications, a chelator that efficiently forms thermodynamically and kinetically stable complexes with them is required. The chelator also needs to attach to a biological targeting vector that locates pathological tissues. Numerous chelators suitable for small radiometals have been established to date, but chelators that work well for large radiometals are significantly less common. In this Account, we describe recent progress by us and others in the advancement of ligands for large radiometal chelation with emerging applications in nuclear medicine.

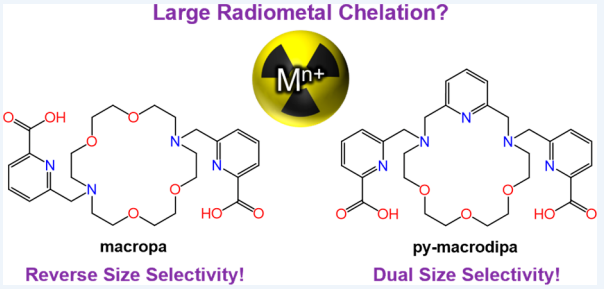


First, we discuss and analyze the coordination chemistry of the chelator macropa, a macrocyclic ligand that contains the 18-crown-6 backbone and two picolinate pendent arms, with large metal ions in the context of nuclear medicine. This ligand is known for its unusual reverse size selectivity, the preference for binding large over small metal ions. The radiolabeling properties of macropa with large radiometals $^{225}Ac^{3+}$, $^{132/135}La^{3+}$, $^{131}Ba^{2+}$, $^{223}Ra^{2+}$, $^{213}Bi^{3+}$, and related in vivo investigations are described. The development of macropa derivatives containing different pendent donors or rigidifying groups in the macrocyclic core is also briefly reviewed.

Next, efforts to transform macropa into a radiopharmaceutical agent via covalent conjugation to biological targeting vectors are summarized. In this discussion, two types of bifunctional analogues of macropa reported in the literature, macropa-NCS and mcp-click, are presented. Their implementation in different radiopharmaceutical agents is discussed. Bioconjugates containing macropa attached to small-molecule targeting vectors or macromolecular antibodies are presented. The in vitro and in vivo evaluations of these constructs are also discussed.

Lastly, chelators with dual size selectivity are described. This class of ligands exhibits good affinities for both large and small metal ions. This property is valuable for nuclear medicine applications that require the simultaneous chelation of both large and small radiometals with complementary therapeutic and diagnostic properties. Recently, we reported an 18-membered macrocyclic ligand called macrodipa that attains this selectivity pattern. This chelator, its second-generation analogue py-macrodipa, and their applications for chelating the medicinally relevant large $^{135}La^{3+}$, $^{225}Ac^{3+}$, $^{213}Bi^{3+}$, and small $^{44}Sc^{3+}$ ions are also presented. Studies with these radiometals show that py-macrodipa can effectively radiolabel and stably retain both large and small radiometals. Overall, this Account makes the case for innovative ligand design approaches for novel emerging radiometal ions with unusual coordination chemistry properties.

## KEY REFERENCES

- Thiele, N. A.; Brown, V.; Kelly, J. M.; Amor-Coarasa, A.; Jermilova, U.; MacMillan, S. N.; Nikolopoulou, A.; Ponnala, S.; Ramogida, C. F.; Robertson, A. K. H.; Rodríguez-Rodríguez, C.; Schaffer, P.; Williams, C., Jr.; Babich, J. W.; Radchenko, V.; Wilson, J. J. An Eighteen-Membered Macrocyclic Ligand for Actinium-225 Targeted Alpha Therapy. *Angew. Chem., Int. Ed.* **2017**, *56*, 14712−14717.[1] *This study reports the effectiveness of the chelator macropa in binding the α-emitter $^{225}Ac^{3+}$. A bifunctional derivative macropa-NCS was developed, and a macropa-based bioconjugate RPS-070 was constructed. In vivo studies revealed the selective uptake of its [$^{225}$Ac]-Ac−RPS-070 complex in a mouse xenograft model of prostate cancer.*
- Hu, A.; MacMillan, S. N.; Wilson, J. J. Macrocyclic Ligands with an Unprecedented Size-Selectivity Pattern

Received: January 3, 2022
Published: March 1, 2022




https://doi.org/10.1021/acs.accounts.2c00003
*Acc. Chem. Res.* 2022, 55, 904−915

for the Lanthanide Ions. *J. Am. Chem. Soc.* **2020**, *142*, 13500−13506.[2] *This work establishes the concept of "dual size selectivity" with two chelators, macrodipa and macrotripa. They show good affinities for both the large and small lanthanide ions by toggling between two distinct conformations.*

- Abou, D. S.; Thiele, N. A.; Gutsche, N. T.; Villmer, A.; Zhang, H.; Woods, J. J.; Baidoo, K. E.; Escorcia, F. E.; Wilson, J. J.; Thorek, D. L. J. Towards the Stable Chelation of Radium for Biomedical Applications with an 18-Membered Macrocyclic Ligand. *Chem. Sci.* **2021**, *12*, 3733−3742.[3] *This work validates macropa as an efffective chelator for $^{223}Ra^{2+}$. Moreover, it reports the in vivo investigation of a $^{223}Ra^{2+}$ radiopharmacetical.*
- Hu, A.; Aluicio-Sarduy, E.; Brown, V.; MacMillan, S. N.; Becker, K. V.; Barnhart, T. E.; Radchenko, V.; Ramogida, C. F.; Engle, J. W.; Wilson, J. J. Py-Macrodipa: A Janus Chelator Capable of Binding Medicinally Relevant Rare-Earth Radiometals of Disparate Sizes. *J. Am. Chem. Soc.* **2021**, *143*, 10429−10440.[4] *A demonstration of the development of the dual-size-selective chelator py-macrodipa and its application in nuclear medicine is presented. Py-macrodipa efficiently forms stable complexes with both large $^{135}La^{3+}$ and small $^{44}Sc^{3+}$.*

## 1. INTRODUCTION

Nuclear medicine is an important branch of radiology that uses ionizing radiation to treat and diagnose diseases. An area of this field that has attracted significant attention within the last two decades is the implementation of internally administered radionuclides in the form of radiopharmaceutical agents.[5−8] Radionuclides that undergo radioactive decay via positron emission, electron capture, or internal conversion are leveraged for diagnostic applications within positron emission tomography (PET) and single-photon emission computed tomography (SPECT). By contrast, radionuclides that emit $\alpha$ particles, $\beta^-$ particles, or Auger electrons are used for therapy. Elements with radioisotopes suitable for nuclear medicine span nearly the entire periodic table.[9−12] In recent years, the diagnostic and therapeutic potentials of large radiometals that reside at the bottom of the periodic table (the fifth period and below) have been recognized. There have been significant efforts to harness them for these applications, as summarized in Table 1.

To transform radiometals into useful therapeutic or diagnostic agents, a chelator is usually required. The chelator serves a critical role in preventing toxicity from the free ions by forming stable metal complexes. These chelators also need to be linked to biological targeting vectors, which selectively target pathological sites. For nuclear medicine, an ideal chelator should address two major challenges. First, it should rapidly incorporate the desired radiometal under mild conditions. Radioactive decay of the radiometal occurs continuously during the radiolabeling process, thereby leading to diminished radiochemical yields if this process is slow. Furthermore, some biological targeting vectors, such as antibodies, are stable only near physiological pH and below 37 °C, thus necessitating mild conditions for radiolabeling. The second criterion is that they form complexes of sufficient thermodynamic and kinetic stability to prevent in vivo radiometal release.[23] Although the kinetic stability is

**Table 1. Large Radiometals Relevant to Nuclear Medicine**

| radiometal | half-life | major decay mode | application | ref |
|---|---|---|---|---|
| $^{132}$La | 4.59 h | $\beta^+$ | PET | 13 |
| $^{134}$La | 6.45 min | $\beta^+$ | PET | 14 |
| $^{135}$La | 18.9 h | electron capture | Auger electron therapy | 15 |
| $^{134}$Ce | 3.16 days | electron capture | PET[a] | 14 |
| $^{225}$Ac | 9.9 days | $\alpha$ | $\alpha$ therapy | 16 |
| $^{212}$Bi | 60.6 min | $\beta^-$, $\alpha$ | $\alpha$ therapy[b] | 17 |
| $^{213}$Bi | 45.6 min | $\beta^-$ | $\alpha$ therapy[b] | 17 |
| $^{131}$Ba | 11.5 days | electron capture | SPECT | 18 |
| $^{223}$Ra | 11.4 days | $\alpha$ | $\alpha$ therapy | 19 |
| $^{212}$Pb | 10.6 h | $\beta^-$ | $\alpha$ therapy[b] | 20 |
| $^{227}$Th | 18.7 days | $\alpha$ | $\alpha$ therapy | 21 |
| $^{230}$U | 20.8 days | $\alpha$ | $\alpha$ therapy | 22 |

[a]$^{134}$Ce is regarded as a PET imaging agent because of its positron-emitting daughter $^{134}$La, despite its decay mode (electron capture). [b]These radionuclides are categorized as $\alpha$-therapy candidates because of their $\alpha$-emitting daughters, despite their major decay modes ($\beta^-$).

challenging to quantify directly, the thermodynamic stability of a metal−ligand coordination complex is readily measured by its stability constant, $K_{ML}$. This constant provides a useful quantitative metric for chelator design efforts.[24] The $K_{ML}$ is defined in eq 1, where [M], [L], and [ML] represent the concentrations of the free metal ions, fully deprotonated ligand, and metal−ligand complex at chemical equilibrium. This constant is pH-independent.

$$K_{ML} = [ML]/[M][L] \quad (1)$$

However, the inherent competition between metal binding and ligand protonation must be considered in assessing the thermodynamic stability. Thus, the ligand basicity, which will affect the conditional stability constant at physiological pH, is another factor that should be considered in these design efforts. For simplicity, our discussions will focus primarily on $K_{ML}$ values, as a sufficient comparator for trends in metal ion selectivity patterns.

To date, nearly all chelators used in clinically approved metal-based radiopharmaceutical agents are derivatives of 1,4,7,10-tetraazacyclododecane-1,4,7,10-tetraacetic acid (DOTA, Chart 1)[25] and diethylenetriaminepentaacetic acid

**Chart 1. Structures of DOTA and DTPA**

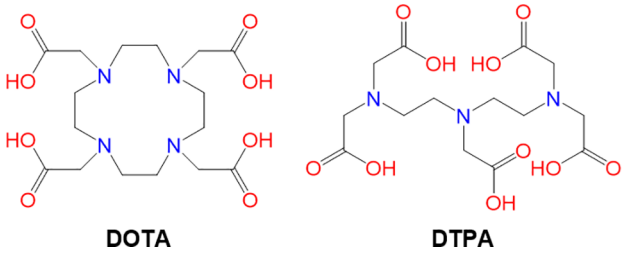


(DTPA, Chart 1). Despite the success of these ligands with smaller ions such as $Lu^{3+}$ and $In^{3+}$, they are significantly less effective for the medicinally valuable large radiometals collected in Table 1. Even though vast research efforts have been devoted to chelator development for nuclear medicine,[11,12,23,26] a majority of these candidates are unsuitable for large radiometals. The scarcity of chelators for large metal ions highlights the inherent challenges associated with their


https://doi.org/10.1021/acs.accounts.2c00003
Acc. Chem. Res. 2022, 55, 904−915


**Figure 1.** Rare earth elements. Spheres are scaled by the 6-coordinate ionic radius[28] of their trivalent cations ($Ln^{3+}$). Their atomic numbers are labeled above.

coordination chemistry. Specifically, the smaller charge densities of large ions weaken their electrostatic interactions with ligands, and their large sizes require unusual ligands that provide a large coordination cavity and multiple donor atoms. Given the great diagnostic and therapeutic potentials of these large radiometals, novel chelation strategies are necessary to effectively harness them.

## 2. CHELATING LARGE METAL IONS WITH MACROPA

To identify and design effective chelators for large metal ions, researchers often investigate their coordination chemistry with rare earth ions ($Ln^{3+}$, Figure 1). All 17 $Ln^{3+}$ ions have similar chemical properties with respect to their oxidation states and ligand donor atom preferences. The only distinguishing feature is their ionic radii, which range from 103.2 pm for $La^{3+}$ to 74.5 pm for $Sc^{3+}$.[27,28] Thus, this class of elements provides a straightforward means of understanding the size selectivity of a chelator. Furthermore, a number of $Ln^{3+}$ ions have valuable medicinal applications.[29] In addition to the rare-earth radionuclides listed in Table 1, $^{149/152/155/161}Tb^{3+}$, $^{86/90}Y^{3+}$, $^{177}Lu^{3+}$, and $^{44/47}Sc^{3+}$ are also relevant to nuclear medicine.[12] $Eu^{3+}$ and $Tb^{3+}$ complexes can be employed as photoluminescent probes,[30] and $Gd^{3+}$ is clinically used in magnetic resonance imaging contrast agents.[31]

The analysis of the $K_{ML}$ values of most chelators for their $Ln^{3+}$ complexes reveals the general trend of a higher affinity for the heavier, smaller $Ln^{3+}$, which is most likely a consequence of their higher charge density that leads to more pronounced metal−ligand electrostatic interactions.[32] This trend is observed for an overwhelming majority of chelators, including extensively used DOTA, DTPA, and ethylenediaminetetraacetic acid (EDTA) (Figure 2a). Chelators with reverse size selectivity, which display a higher affinity for large $Ln^{3+}$, are rare.

Because of recent interest in the large radiometals for nuclear medicine applications, there has been an impetus to find chelators that exhibit reverse size selectivity. Early studies identified chelators based on the 4,13-diaza-18-crown-6 macrocyclic core to possess a preference for large $Ln^{3+}$. For instance, odda (Chart 2, Figure 2b) shows a greater affinity for large $Ln^{3+}$ ions, albeit with a modest selectivity across the series ($\log K_{CeL} - \log K_{LuL} = 1.4$).[37] Its analogue oddm also prefers large $Ln^{3+}$, but with a greater selectivity ($\log K_{CeL} - \log K_{LuL} = 5.4$).[40] These studies indicated that the 4,13-diaza-18-crown-6 macrocycle potentially confers this unusual selectivity.

In 2009, the chelator macropa or bp18c6, a derivative of the 4,13-diaza-18-crown-6 macrocycle with two pendent picolinate arms, was also shown to be reverse-size-selective (Figure 2b), with an unprecedented ability to discriminate between large and small $Ln^{3+}$ ($\log K_{CeL} - \log K_{LuL} = 6.9$).[38] Its large $Ln^{3+}$ complexes exhibit excellent thermodynamic and kinetic stability. The $La^{3+}$−macropa complex has a $\log K_{LaL} = 14.99$[38] and is kinetically stable for 3 weeks in the presence of 1000 equiv of DTPA at pH 7.4.[1] Crystal structures of the $La^{3+}$ and $Lu^{3+}$ macropa complexes (Figure 3a,b) provide

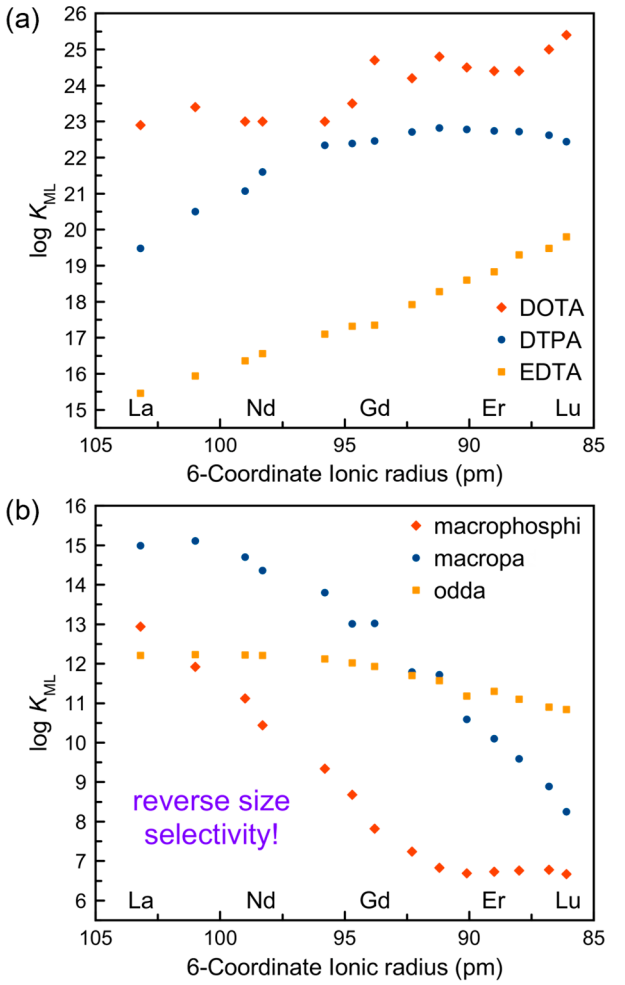


**Figure 2.** $K_{ML}$ values of $Ln^{3+}$ complexes formed with (a) DOTA, DTPA, EDTA and (b) odda, macropa, macrophosphi plotted versus ionic radii. Data are obtained from refs 33−39.

insight into the reverse size selectivity of this ligand. Even though both complexes attain distorted $C_2$ symmetry, notable disparities in the interatomic distances are found within these two structures. For example, La−N1 and La−N2 distances are 0.04 Å from each other, whereas the Lu−N1 and Lu−N2 distances differ by 0.10 Å, indicating a greater degree of asymmetry for the latter. Furthermore, the 18-crown-6 scaffold in the $Lu^{3+}$ complex is significantly more puckered than that in the $La^{3+}$ complex, signifying a higher ligand strain for the former, as also supported by computational studies.[41] These observations indicate that the 4,13-diaza-18-crown-6 macrocyclic backbone is optimally suited for interacting with large ions such as $La^{3+}$. Other computational studies on macropa metal-binding properties also provided insight on its selectivity by noting a subtle balance between the metal−ligand binding energy and the $Ln^{3+}$ hydration energy.[42] Moreover, the reverse size selectivity of macropa extends to other classes of metal


https://doi.org/10.1021/acs.accounts.2c00003
Acc. Chem. Res. 2022, 55, 904−915

**Chart 2. Structures of Odda, Oddm, and Macropa**

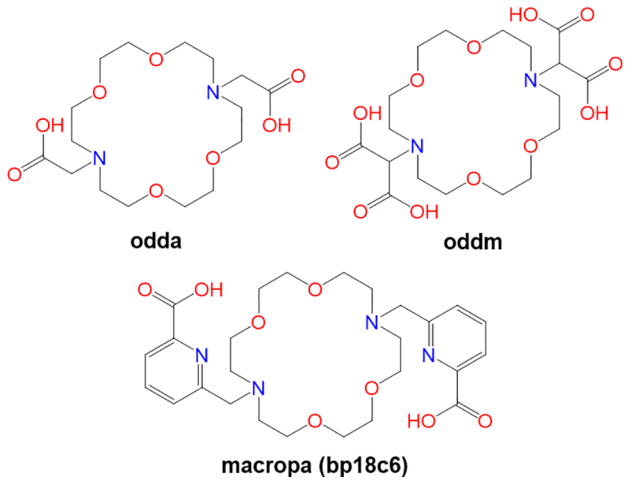


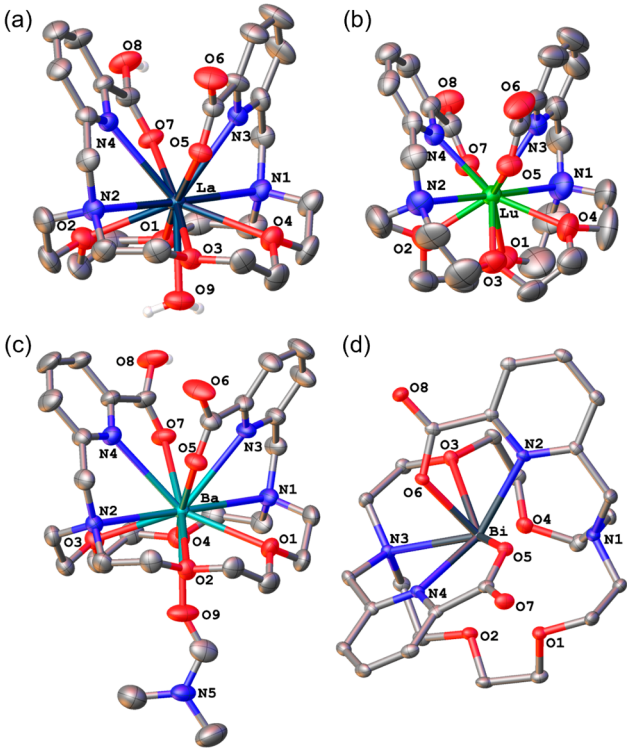


**Figure 3.** Crystal structures of (a) $[La(Hmacropa)(OH_2)]^{2+}$, (b) $[Lu(macropa)]^{+}$, (c) $[Ba(Hmacropa)(DMF)]^{+}$, and (d) $[Bi(macropa)]^{+}$. Counterions, nonacidic hydrogen atoms, and outer-sphere solvent molecules are omitted for clarity. Crystallographic data are from refs 1, 44, and 45.

ions such as the alkaline earths, where the $K_{ML}$ trend is $K_{BaL} > K_{SrL} > K_{CaL}$.[43,44]

The pronounced reverse size selectivity of macropa prompted us to explore its ability to chelate large radiometals for nuclear medicine applications. Our particular interest when we initiated this project five years ago was the therapeutic $\alpha$-emitting $^{225}Ac^{3+}$.[16] Its conjugation to appropriate biological targeting vectors required the use of DOTA, necessitating either a two-step radiolabeling process[46] or a long incubation because of the slow binding kinetics of this ligand.[47] Given the high affinity of macropa for $La^{3+}$ and the chemical similarity of $La^{3+}$ and $Ac^{3+}$,[48] we reasoned that macropa would be an effective chelator for this promising therapeutic radiometal. In line with this expectation, we discovered that macropa quantitatively complexed $^{225}Ac^{3+}$ within 5 min at RT and pH 5.5−6 at sub-$\mu$M ligand concentration, surpassing the high-temperature conditions required for DOTA. To evaluate the in vivo stability of the $[^{225}Ac][Ac(macropa)]^{+}$ complex, we performed biodistribution studies in C57BL/6 mice, using $[^{225}Ac]Ac(NO_3)_3$ as the control. The biodistribution profile of $[^{225}Ac]Ac(NO_3)_3$ shows slow blood clearance with accumulation occurring in the liver and spleen (Figure 4a). By

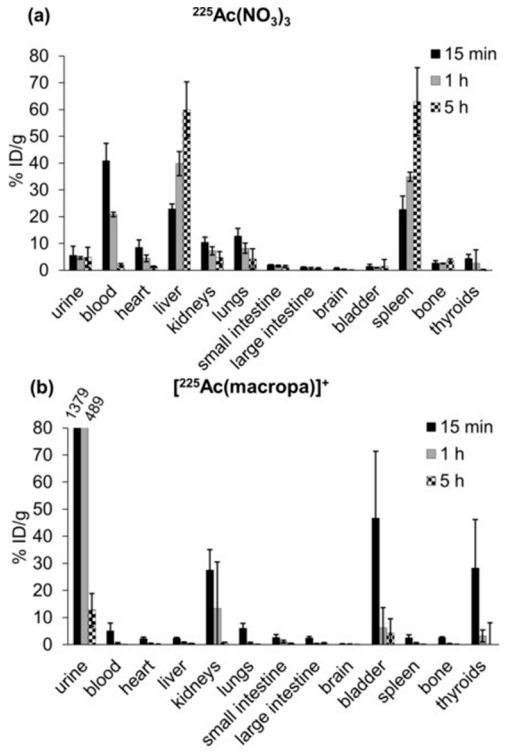


**Figure 4.** Biodistribution of (a) $[^{225}Ac]Ac(NO_3)_3$ and (b) $[^{225}Ac][Ac(macropa)]^{+}$ following intravenous injection in adult C57BL/6 mice. The numbers written over "urine" are their measured %ID $g^{-1}$, which are off-scale compared to the %ID $g^{-1}$ values for other organs. Adapted with permission from ref 1. Copyright 2017 Wiley-VCH Verlag GmbH & Co. KGaA.

contrast, $[^{225}Ac][Ac(macropa)]^{+}$ was rapidly excreted from the mice, affording negligible residual activity in these organs (Figure 4b). This distinction indicates that $[^{225}Ac][Ac(macropa)]^{+}$ does not release free $^{225}Ac^{3+}$ in vivo.[1] Thus, the rapid radiolabeling kinetics and excellent in vivo stability revealed macropa to be a highly promising chelator for $^{225}Ac^{3+}$ therapy.

We next investigated macropa for medicinally relevant radioisotopes of $La^{3+}$. In particular, the $^{132/135}La^{3+}$ pair can be used for PET imaging and Auger electron therapy.[15,49] Like $Ac^{3+}$, the large ionic radius of $La^{3+}$ makes conventional chelators such as DOTA and DTPA poorly effective. In our radiolabeling studies, we found that macropa complexed $^{132/135}La^{3+}$ with a high apparent molar activity (4.34 Ci·$\mu$mol$^{-1}$) at RT and pH 5.5 within 30 min. By contrast, even at an elevated temperature (80 °C), DOTA reached a molar activity of only 0.67 Ci·$\mu$mol$^{-1}$.[50]

$^{223}Ra^{2+}$, another promising large therapeutic radiometal, is currently the only $\alpha$-particle emitter approved for clinical use



https://doi.org/10.1021/acs.accounts.2c00003
Acc. Chem. Res. 2022, 55, 904−915

in the form of unchelated [$^{223}$Ra]$RaCl_2$, which is applied for the management of bone metastases in castration-resistant prostate cancer patients.[51] As the largest divalent cation in the periodic table (8-coordinate ionic radius of 148 pm),[28] the identification of suitable chelators for $^{223}Ra^{2+}$ has been significantly hindered. In this context, we established that macropa has a high affinity for $Ba^{2+}$, the lighter congener of $Ra^{2+}$, forming a complex with geometry analogous to that of $La^{3+}$ (Figure 3c). Macropa is thus a potent dissolution agent for barite scale, which is a problem of significance in the petroleum industry.[44] Furthermore, macropa was recently evaluated for the chelation of diagnostic $^{131}Ba^{2+}$ by others. Within an hour, macropa quantitatively radiolabeled $^{131}Ba^{2+}$ at RT and pH 6 at a ligand concentration of $10^{-4}$ M. The resulting radiometal complex did not dissociate after 3 days in human serum at 37 °C.[52]

Thus, we sought to explore macropa as a potential candidate for $^{223}Ra^{2+}$ complexation. Consistent with its $Ba^{2+}$-binding properties, macropa formed the [$^{223}$Ra][Ra(macropa)] complex quantitatively within 5 min at RT and pH 6, and the ligand concentration required for 50% radiolabeling efficiency was determined to be 13 $\mu$M. Importantly, [$^{223}$Ra][Ra(macropa)] remained ~90% intact in human serum at 37 °C after 12 days.[3] In vivo mouse studies comparing [$^{223}$Ra][Ra(macropa)] and [$^{223}$Ra]$RaCl_2$ revealed distinct biodistribution properties. Consistent with the osteophilic property of $Ra^{2+}$,[53] [$^{223}$Ra]$RaCl_2$ accumulated in bone (Figure 5a), whereas the bone uptake of $^{223}Ra^{2+}$ was markedly reduced within mice injected with [$^{223}$Ra][Ra(macropa)] (Figure 5b). The intestine and spleen uptake were also significantly decreased. These substantial differences suggest that [$^{223}$Ra][Ra(macropa)] remains intact in vivo.[3]

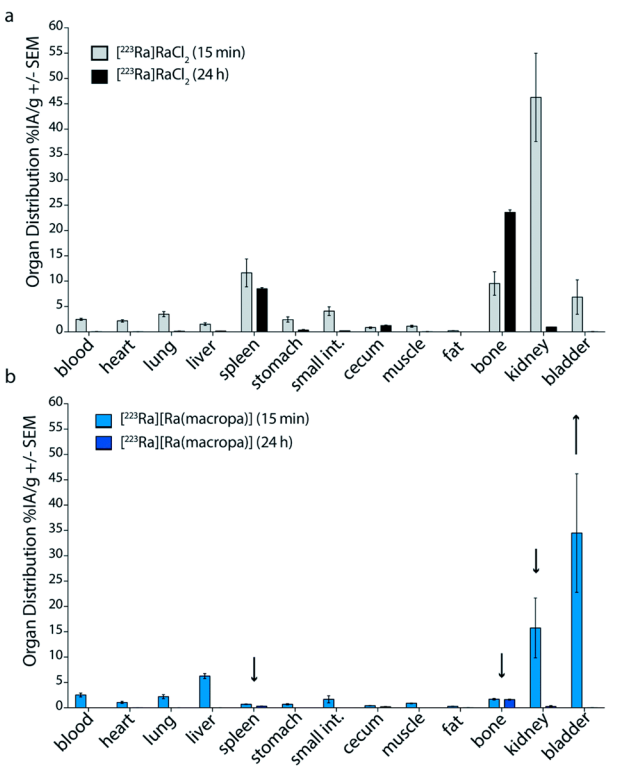


**Figure 5.** Biodistribution of (a) [$^{223}$Ra]$RaCl_2$ and (b) [$^{223}$Ra][Ra(macropa)] in healthy, skeletally mature mice sacrificed 15 min and 24 h after injection. Adapted with permission from ref 3. Copyright 2021 Royal Society of Chemistry.

As the most recent example, we investigated the coordination chemistry of macropa with $Bi^{3+}$ and its suitability for therapeutic $\alpha$-emitting $^{213}Bi^{3+}$. Unlike the s- and f-block metal ions discussed above, $Bi^{3+}$ usually forms coordination complexes with anisotropic coordination spheres as a result of the stereochemical activity of the $6s^2$ lone pair.[54,55] The crystal structure of $[Bi(macropa)]^+$ is notably different from those of the $La^{3+}$, $Lu^{3+}$, and $Ba^{2+}$ complexes (Figure 3). The $Bi^{3+}$ center sits asymmetrically within the coordination sphere, and the macrocyclic donor atoms do not fully engage with $Bi^{3+}$, a consequence of the $Bi^{3+}$ $6s^2$ stereochemical activity. In the radiolabeling studies, macropa efficiently complexed $^{213}Bi$ within 8 min at RT and pH 5.5−6 at a ligand concentration of $\geq 10^{-6}$ M.[45] Collectively, macropa has proven to be an effective chelator for large radiometals including several promising $\alpha$-emitting radionuclides.

On account of the efficacy of macropa, we and others have been investigating analogues of this ligand. Macropa was altered either by varying the pendent donors (macropaquin, macroquin-$SO_3$, macrophospho, and macrophosphi; Chart 3)[39,44,45,56] or by modifying the macrocyclic backbone (CHX-macropa and BZ-macropa; Chart 3).[41,57] Notably, macroquin-$SO_3$ forms a highly kinetically stable complex with $Bi^{3+}$, suggesting its promise for $^{213}Bi^{3+}$ chelation.[45] Moreover, macrophosphi retains its reverse size selectivity but differs from macropa in its pronounced ability to discriminate light $Ln^{3+}$ ions (Figure 2b). This property was leveraged for an effective liquid−liquid extraction separation between adjacent early $Ln^{3+}$ ions $La^{3+}$ and $Ce^{3+}$.[39]

**Chart 3. Structures of Macropa Derivatives Discussed in This Manuscript**

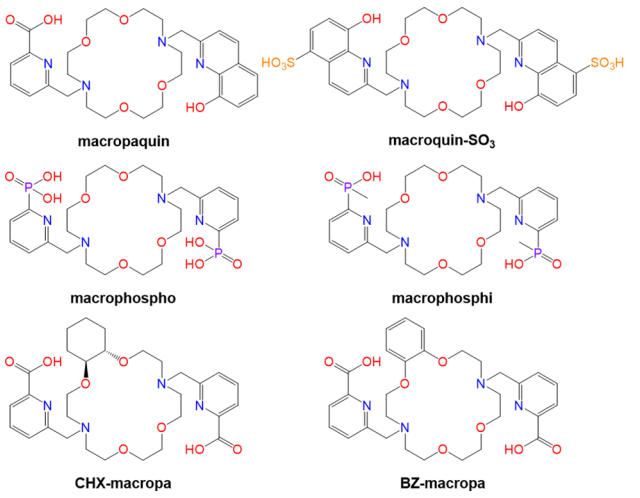


## 3. DEVELOPMENT OF MACROPA-BASED BIFUNCTIONAL CHELATORS AND BIOCONJUGATES FOR RADIOPHARMACEUTICAL APPLICATIONS

As highlighted above, macropa is an effective chelator for large radiometals with relevance to nuclear medicine. For actual radiopharmaceutical applications, however, they need to be conjugated to biological targeting vectors such as peptides, antibodies, polysaccharides, or lipids, which selectively target


https://doi.org/10.1021/acs.accounts.2c00003
Acc. Chem. Res. 2022, 55, 904−915

pathological locations. For this purpose, bifunctional chelators, which contain both the metal-binding component and a reactive functional group, are needed. This reactive group can form covalent bonds with biomolecules, giving rise to a bioconjugate (Figure 6) that can be directly used in radiopharmaceutical contexts.[5,58]

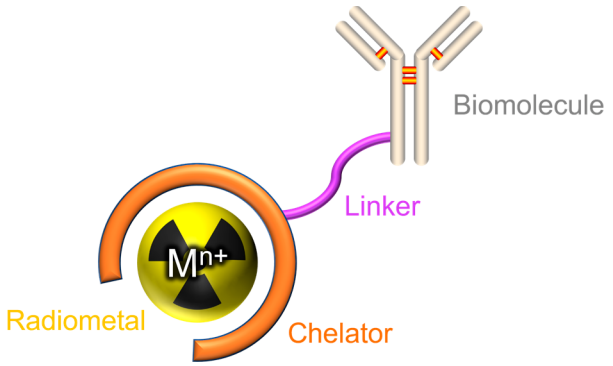


**Figure 6.** Schematic representation of a bioconjugate used for nuclear medicine.

To take advantage of the effective radiometal-binding properties of macropa, a bifunctional analogue, macropa-NCS (Chart 4a), was prepared via an eight-step organic synthesis.[1] The isothiocyanate group (−NCS), which reacts with a primary amine to form a thiourea linkage,[59] was introduced. Macropa-NCS was then successfully conjugated to a small molecule, giving a bioconjugate RPS-070 (Chart 4b). It contains a "Lys−urea−Glu" moiety, which targets the prostate-specific membrane antigen (PSMA) that is overexpressed in prostate cancer.[60] In addition, a serum-albumin-binding iodophenyl group was also included to prolong in vivo circulation.[61] Like free macropa, RPS-070 rapidly incorporated $^{225}Ac^{3+}$ within 20 min at RT and pH 5−5.5, demonstrating that the newly introduced biomolecule does not negatively affect the coordination properties of this ligand. Furthermore, the radiometal complex [$^{225}$Ac]Ac−RPS-070 shows significant uptake in the tumors of mice bearing LNCaP (PSMA+ prostate cancer) xenografts with no other apparent off-target accumulation. However, $^{225}$Ac−RPS-070 exhibited fast renal clearance as marked by a significant loss of radioactivity within 4 h.[1]

To extend the in vivo circulation of RPS-070, an analogue of this compound, RPS-074 (Chart 4b), was prepared by modifying the length of the PEG-linking units between macropa, the PSMA-targeting moiety, and the albumin-binding iodophenyl group. Like macropa and RPS-070, RPS-074 rapidly binds to and forms a stable complex with $^{225}Ac^{3+}$. In contrast to [$^{225}$Ac]Ac−RPS-070, the circulation of [$^{225}$Ac]Ac−RPS-074 is significantly longer, resulting in a larger and more prolonged accumulation in the LNCaP prostate tumor xenografts in mice (Figure 7a). Although a clear dose−response relationship was not apparent in these studies as a result of challenges with tumor size heterogeneity, all administered doses at the beginning of a 75-day therapy study resulted in significantly retarded tumor growth and an increased survival of mice over the experiment duration compared to the vehicle-treated control (Figure 7b).[62]

Macropa-NCS was also conjugated to the monoclonal antibody, trastuzumab, and the resulting chelator-antibody construct was labeled with $^{225}Ac^{3+}$.[1] In subsequent work by others, macropa-NCS was attached to the humanized monoclonal IgG1 antibody GC33,[63] which binds to the protein glypican-3 that is highly expressed in liver cancer.[64] Like the macropa-trastuzumab conjugate, macropa-GC33 was effective at complexing and retaining $^{225}Ac^{3+}$, as >95% of it remained intact after being incubated in human serum for 14 days at 37 °C. [$^{225}$Ac]Ac−macropa-GC33 was further evaluated in mice bearing liver cancer HepG2 tumor xenografts. Its biodistribution revealed substantial tumor uptake (12.9% ID·g$^{-1}$ at 48 h and 12.0% ID·g$^{-1}$ at 144 h postinjection), consistent with the liver-cancer-targeting property of GC33. Furthermore, [$^{225}$Ac]Ac−macropa-GC33 was able to prolong the survival of these mice compared to the untreated control, providing further support for the use of macropa in radiopharmaceutical therapy.[63]

We also applied macropa-NCS with a smaller PSMA-targeting moiety called DUPA to assess this bifunctional chelator for $^{132/135}La^{3+}$ and $^{223}Ra^{2+}$. This bioconjugate, macropa-DUPA (Chart 4b), was tested with $^{132/135}La^{3+}$, revealing quantitative radiolabeling within 30 min at RT and pH 5.5. [$^{132/135}$La]La−macropa-DUPA was then assessed in mice bearing two implanted tumor xenografts, comprising PSMA+ (PC3-PIP) and PSMA− (PC3-flu) cells. PET/CT scans on these mice revealed a significant uptake of the radiotracer only in the PSMA+ xenograft at both 1 and 4 h postinjection (Figure 8), and this result was further verified by ex vivo biodistribution studies.[50] This study signified the first example of employing $La^{3+}$ radioisotopes for radiopharmaceutical imaging.

Subsequently, we evaluated macropa-DUPA with $^{223}Ra^{2+}$. Consistent with studies on the unfunctionalized macropa, macropa-DUPA efficiently incorporated $^{223}Ra^{2+}$, and the resulting complex remained >90% intact after 12 days in human serum at 37 °C. However, the biodistribution of [$^{223}$Ra]Ra−macropa-DUPA revealed significant bone uptake matching that of [$^{223}$Ra]$RaCl_2$, suggesting that [$^{223}$Ra]Ra−macropa-DUPA is unstable in vivo, in stark contrast to the in vivo stability observed for [$^{223}$Ra][Ra(macropa)].[3] These observations highlight an important but scarcely understood phenomenon: the biological targeting vector can have a profound effect on complex stability.

Despite the value of macropa-NCS as a bifunctional chelator, its vulnerability to hydrolysis limits its potential. The electron-withdrawing nature of the picolinate makes the −NCS functional group significantly more reactive. For example, compared to the bifunctional DOTA, *p*-NCS-Bn-DOTA (Chart 4a), which contains the −NCS group on a phenyl group, macropa-NCS undergoes hydrolysis 10 times faster.[1] Thus, the development of alternative, more bench-stable bifunctional analogues of macropa is desirable. In this context, mcp-M-click and mcp-D-click (Chart 4c) were recently reported.[65] The more stable alkyne groups in these ligands can undergo the copper-catalyzed azide−alkyne cycloaddition (CuAAC) click reaction.[59,66] Leveraging this chemistry, these ligands were successfully conjugated to an azide-containing PSMA-targeting peptide, yielding mcp-M-PSMA and mcp-D-PSMA. Both bioconjugates retained excellent radiolabeling efficiencies with $^{225}Ac^{3+}$. In particular, [$^{225}$Ac]Ac−mcp-D-PSMA exhibited a high binding affinity for PSMA and effectively inhibited the growth of LNCaP cells in an in vitro colony-formation assay. Lastly, biodistribution studies of both bioconjugates in mice bearing LNCaP tumors revealed them to preferentially accumulate in the tumors.[65]


https://doi.org/10.1021/acs.accounts.2c00003
Acc. Chem. Res. 2022, 55, 904−915

**Chart 4. Bifunctional Chelators and Bioconjugates Discussed in this Manuscript**[a]

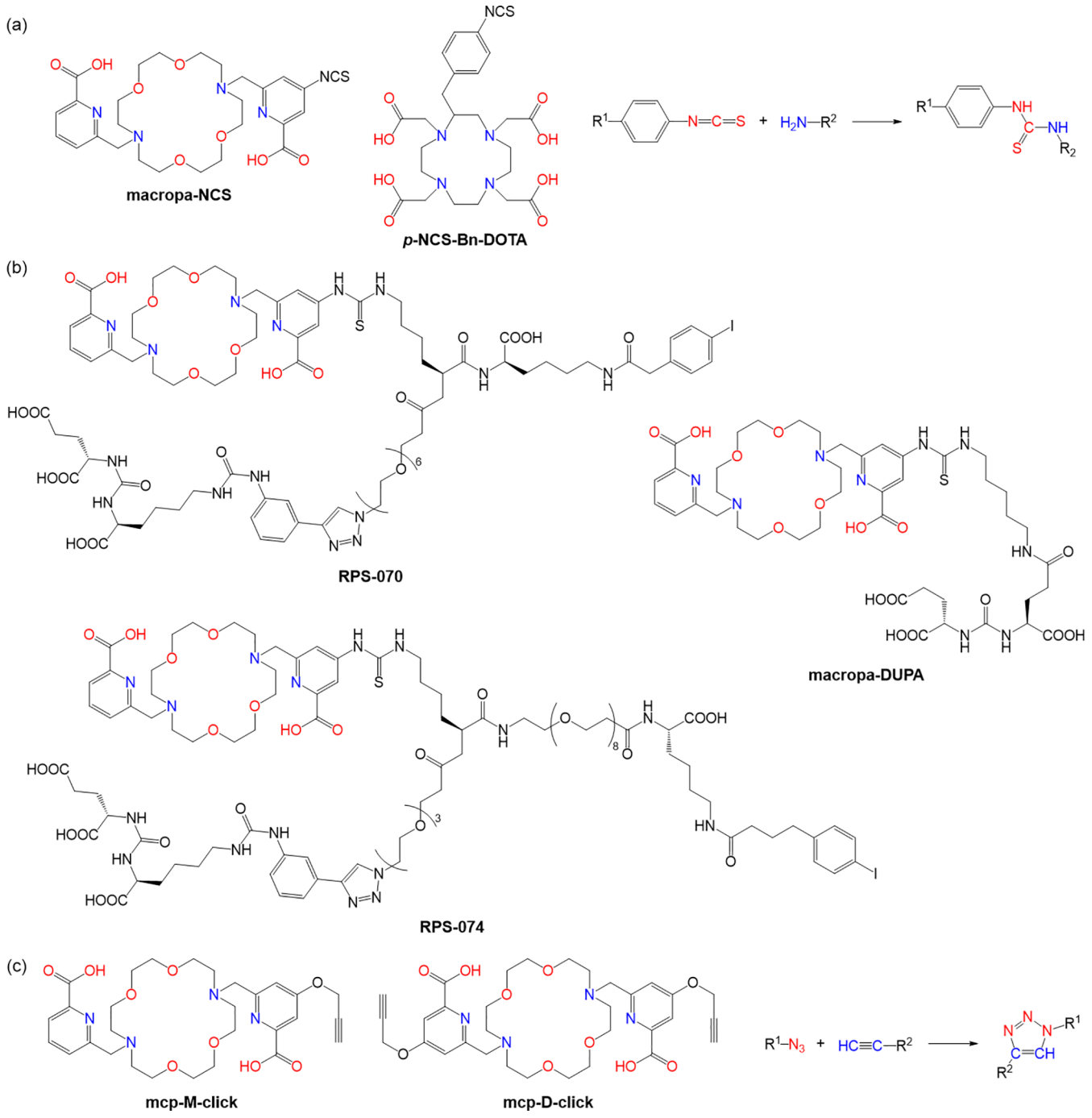


[a](a) Structures of bifunctional chelators macropa-NCS, *p*-NCS-Bn-DOTA, and their corresponding conjugation reaction. (b) Structures of bioconjugates RPS-070, RPS-074, and macropa-DUPA. (c) Structures of bifunctional chelators mcp-M-click, mcp-D-click, and their corresponding conjugation reaction.

## 4. STABLE CHELATION FOR BOTH THE LARGE AND SMALL METAL IONS: THE "MACRODIPA-TYPE" CHELATORS AND THEIR DUAL SIZE SELECTIVITY

A key limitation of macropa is its ineffectiveness for smaller radiometal ions. This property is concerning because most metallic radionuclides currently used in nuclear medicine are smaller ions, such as diagnostic radiometals $^{68}Ga^{3+}$, $^{111}In^{3+}$, and $^{44}Sc^{3+}$, which are unamenable to macropa chelation.[67] In situations where large and small radiometals are needed simultaneously, such as for theragnostic purposes, a chelator system that effectively binds both types of metal ions would be valuable. In addition, chelating both large and small ions with a single ligand is more beneficial than using two distinct structures. Two metal complexes arising from the same ligand should have comparable chemical properties that manifest in similar in vivo biodistribution and circulation times, which is critical for theragnostics.

Toward this goal, we reported a macrocyclic chelator macrodipa (Chart 5) that shows an unprecedented dual size


https://doi.org/10.1021/acs.accounts.2c00003
Acc. Chem. Res. 2022, 55, 904−915

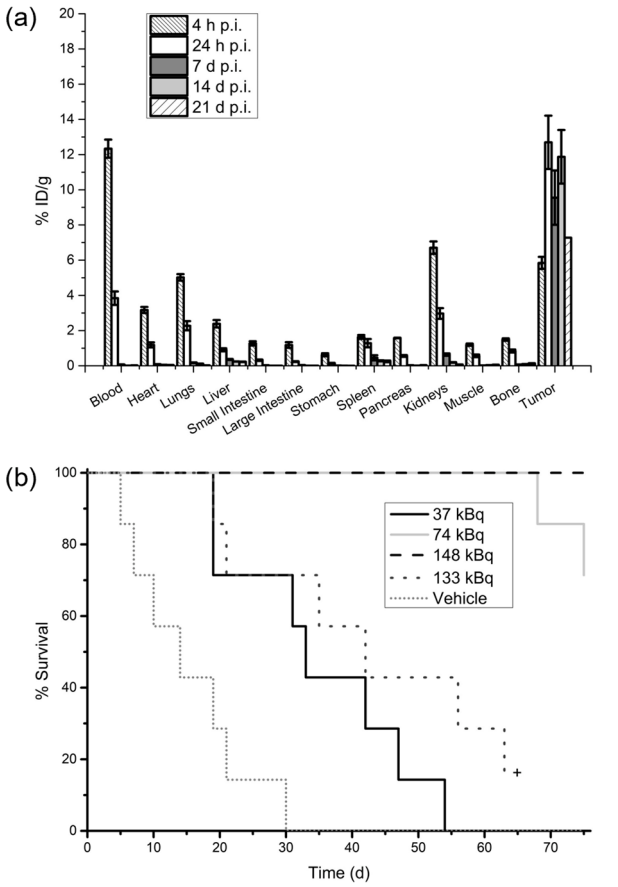


**Figure 7.** (a) Biodistribution of [$^{225}$Ac]Ac−RPS-074 following intravenous injection in male BALB/c *nu/nu* mice bearing LNCaP xenograft tumors. (b) Kaplan−Meier plot comparing the survival of male BALB/c *nu/nu* mice bearing LNCaP xenograft tumors treated with different doses of [$^{225}$Ac]Ac−RPS-074. Reproduced with permission from ref 62. Copyright 2019 Society of Nuclear Medicine and Molecular Imaging.

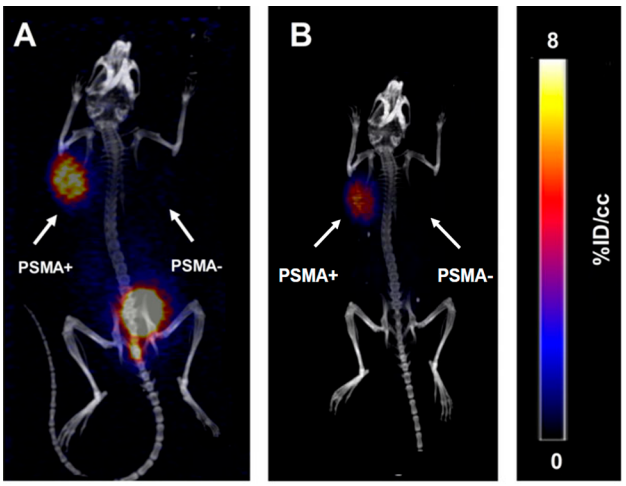


**Figure 8.** Representative PET/CT images of mice bearing PC3-PIP/flu tumors (A) 1 and (B) 4 h after the injection of [$^{132/135}$La]La−macropa−DUPA. Adapted with permission from ref 50. Copyright 2019 Wiley-VCH Verlag GmbH & Co. KGaA.

selectivity for the $Ln^{3+}$ ions. As shown in Figure 9a, macrodipa exhibits better affinities for both the large and small $Ln^{3+}$ ions.[2] Crystallographic analysis of its $La^{3+}$ and $Lu^{3+}$ complexes

**Chart 5. Structures of Macrodipa, Py-Macrodipa, Oxyaapa, and Pypa**

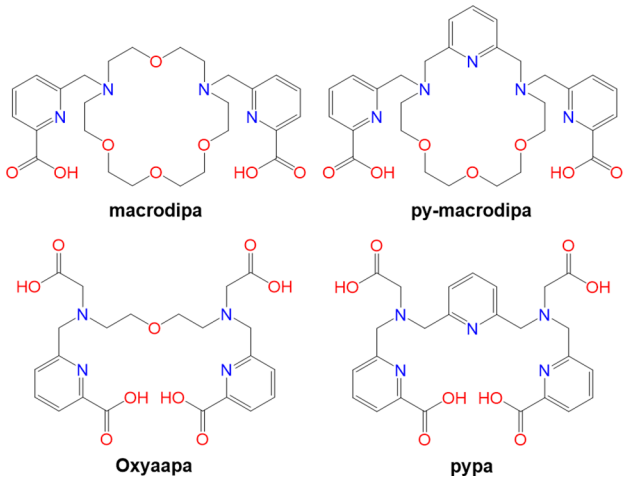


(Figure 9b) revealed that macrodipa attains two distinct conformations in binding large ions such as $La^{3+}$ and small ions such as $Lu^{3+}$. Upon binding $La^{3+}$, a 10-coordinate, nearly $C_2$-symmetric complex forms in which all six donor atoms on the macrocyclic backbone interact with the metal (Conformation A). By contrast, in the $Lu^{3+}$ structure, three of the oxygen atoms present within the macrocycle do not directly engage with the central ion, resulting in an 8-coordinate, asymmetric complex (Conformation B). In addition to X-ray crystallography, comprehensive NMR spectroscopic studies verified the presence of these two distinct conformations in solution. Furthermore, DFT calculations revealed that Conformation A is energetically favored for large ions but Conformation B is more stable for small ions. Thus, the unique dual size selectivity of macrodipa arises from its conformational toggle that enables the accommodation of both large and small metal ions.[2]

Despite this novel selectivity pattern, the $Ln^{3+}$ complexes of macrodipa are labile, as reflected by their instability to transchelation by DTPA.[4] This lability precludes the use of macrodipa for nuclear medicine, thus prompting us to pursue alternative but related ligand design strategies. It has been demonstrated that the installation of pyridyl donors, in place of ethereal oxygen donors, augments complex stability. The pyridine-containing pypa, for example, represents an improvement over Oxyaapa (Chart 5).[68,69] Following this lead, we targeted a macrodipa analogue, py-macrodipa (Chart 5), which replaces one of the ethereal oxygen donors with a pyridyl moiety.[4] As plotted in Figure 9a, this modification led to a significant enhancement of the thermodynamic stability of its $Ln^{3+}$ complexes without compromising its dual-size-selectivity profile. As for macrodipa, a suite of X-ray crystallographic (Figure 10a), NMR spectroscopic, and DFT studies verified that py-macrodipa achieves this selectivity pattern by accommodating both large and small ions in different Conformations A and B. Importantly, the kinetic stability of the $Ln^{3+}$ complexes of py-macrodipa is also considerably greater than that of macrodipa complexes. This enhanced kinetic stability is most likely a consequence of the additional rigidity introduced by the planar pyridyl unit as well as its stronger donor strength.[4]

Given the enhanced complex stability of py-macrodipa, its potential for nuclear medicine was assessed. To capitalize on


https://doi.org/10.1021/acs.accounts.2c00003
Acc. Chem. Res. 2022, 55, 904−915

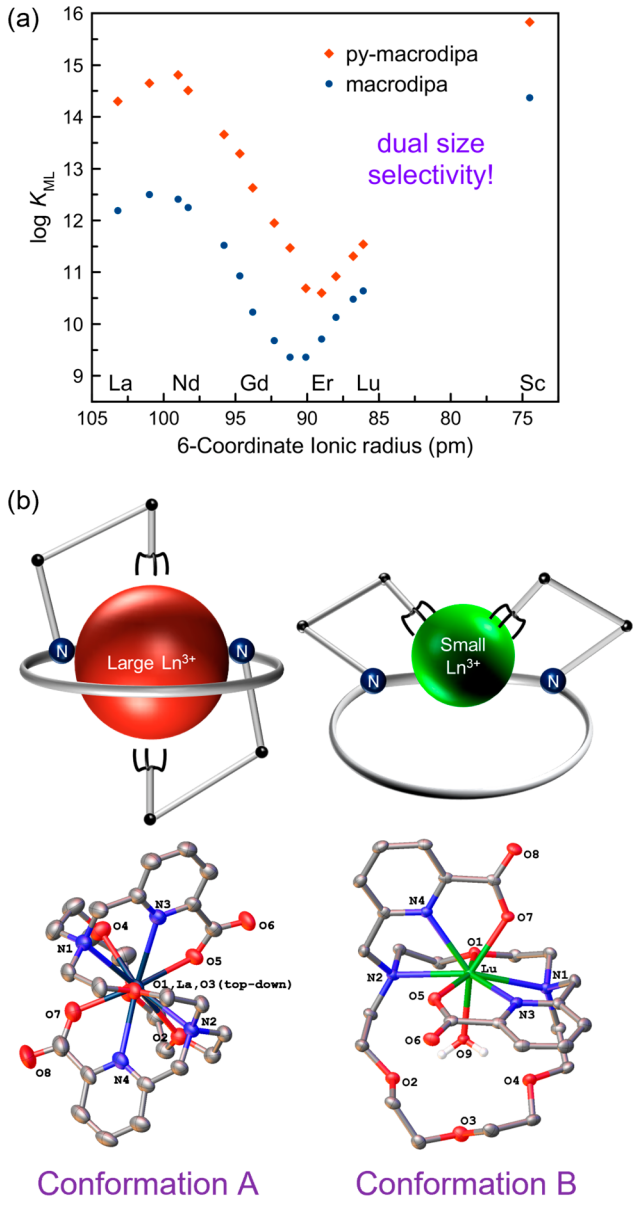


**Figure 9.** (a) $K_{ML}$ values of $Ln^{3+}$ complexes formed with macrodipa and py-macrodipa plotted versus ionic radii. (b) Illustration of the conformational toggle in macrodipa that occurs during complexation with large and small $Ln^{3+}$ ions, as verified by representative crystal structures of [La(macrodipa)]$^+$ and [Lu(macrodipa)$(OH_2)$]$^+$. Data are adapted from refs 2 and 4.

its dual size selectivity, two radiometals that represent the maximum and minimum ionic radii within the $Ln^{3+}$ series, $^{135}La^{3+}$ and $^{44}Sc^{3+}$, were chosen. $^{135}La^{3+}$ is a promising Auger electron emitter that is valuable for therapeutic purposes, whereas $^{44}Sc^{3+}$ is a diagnostic positron emitter. The significant size difference of these ions requires different chelators. For example, $Sc^{3+}$ is effectively complexed by DOTA, whereas the corresponding $La^{3+}$ complex is significantly less stable. Likewise, macropa is a good ligand for $La^{3+}$ but works poorly for $Sc^{3+}$. Remarkably, py-macrodipa radiolabeled both $^{135}La^{3+}$ and $^{44}Sc^{3+}$ at RT and pH 5.5 within 15 min with high apparent molar activities. Furthermore, both radiometal complexes were stable in human serum at 37 °C, showing no noticeable dissociation over a timescale that matches their physical half-lives (Figure 10b).[4] These results highlight the effectiveness of

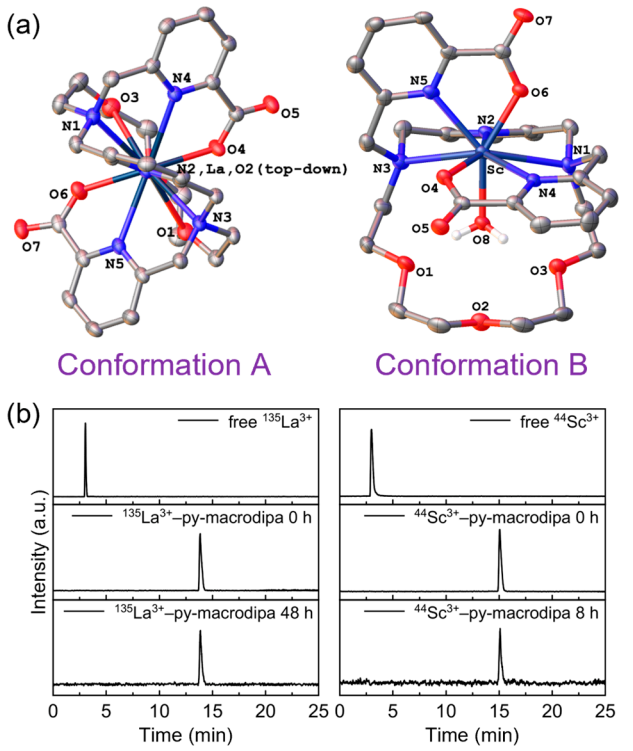


**Figure 10.** (a) Crystal structures of [La(py-macrodipa)]$^+$ and [Sc(py-macrodipa)$(OH_2)$]$^+$, which represent Conformations A and B, respectively. (b) Human serum challenge assay for [$^{135}$La][La(py-macrodipa)]$^+$ and [$^{44}$Sc][Sc(py-macrodipa)$(OH_2)$]$^+$ complexes, as monitored by radio-HPLC. Data are adapted from ref 4.

py-macrodipa for chelating both the large and small radiometal ions. The clever design strategies applied for py-macrodipa demonstrate the proof-of-principle possibility of developing chelators that can be adopted for radionuclides with disparate ionic radii.

On the basis of the success of py-macrodipa with $^{135}La^{3+}$ and $^{44}Sc^{3+}$, we next employed this system for other non-$Ln^{3+}$ radiometals such as large $\alpha$-emitting radiometals $^{225}Ac^{3+}$ and $^{213}Bi^{3+}$. Despite the nearly identical ionic radii of $La^{3+}$ and $Bi^{3+}$,[28] the $Bi^{3+}$ complex of py-macrodipa adopts asymmetric Conformation B,[70] which is normally preferred for small ions. This unexpected geometry is possibly a consequence of the stereochemical activity of the $Bi^{3+}$ $6s^2$ lone pair.[54,55] Both $^{225}Ac^{3+}$ and $^{213}Bi^{3+}$ were efficiently incorporated by py-macrodipa at RT and pH 5.5−6, and quantitative radiolabeling was observed for $^{225}Ac^{3+}$ and $^{213}Bi^{3+}$ at ligand concentrations of $\geq 10^{-5}$ and $\geq 10^{-7}$ M, respectively. Even though the py-macrodipa complex with $Ac^{3+}$ is kinetically labile and not optimal for nuclear medicine purposes, the $Bi^{3+}$ complex has remarkable kinetic stability, surpassing that of macropa.[70] This study established py-macrodipa as a promising candidate for $^{213}Bi^{3+}$ chelation, representing an extension of its versatility for a wide range of metal ions.

## 5. CONCLUSIONS AND OUTLOOK

Within recent years, the therapeutic and diagnostic properties of radioisotopes of large metal ions have been recognized for their potential in nuclear medicine. The coordination chemistry of these ions, however, is less developed than those of other more commonly used radionuclides, thus necessitating the advancement of novel chelator systems. In


https://doi.org/10.1021/acs.accounts.2c00003
Acc. Chem. Res. 2022, 55, 904−915

this Account, we have reviewed the efforts by us and others in the last five years to address this challenge.

As we have demonstrated, macropa and its bifunctional analogues have high promise for chelating large ions, showing significant advantages over the prior state-of-the-art ligand DOTA. In addition, modifying the 18-membered macrocycle affords a new class of macrodipa-type chelators exhibiting dual size selectivity, which may be valuable for theragnostic applications. Understanding fundamental coordination chemistry and applying that knowledge to clever ligand design approaches are critical in this regard.

There are still significant challenges that will require more effort in this area. For example, the successful targeting of $^{223}Ra^{2+}$ to tumors has not yet been demonstrated. We also envision that expanding the dual size selectivity concept to specifically match the ionic radii of desired theragnostic radionuclide pairs will be of significant clinical interest and value. Inorganic and coordination chemists have a unique skill set for making key advances in the field of nuclear medicine.

## AUTHOR INFORMATION


### Corresponding Author

**Justin J. Wilson** − *Department of Chemistry and Chemical Biology, Cornell University, Ithaca, New York 14853, United States;* orcid.org/0000-0002-4086-7982; Email: jjw275@cornell.edu

### Author

**Aohan Hu** − *Department of Chemistry and Chemical Biology, Cornell University, Ithaca, New York 14853, United States;* orcid.org/0000-0002-9720-3159

Complete contact information is available at: https://pubs.acs.org/10.1021/acs.accounts.2c00003


### Notes

The authors declare no competing financial interest.

### Biographies

**Aohan Hu** is a Ph.D. candidate in the Department of Chemistry and Chemical Biology at Cornell University. He grew up in Yueyang, Hunan, China and received his B.S. in chemistry from Wuhan University (2017). His current research is focused on chelator design for heavy metal ions and the medicinal applications of their coordination compounds.

**Justin J. Wilson** is an associate professor in the Department of Chemistry and Chemical Biology at Cornell University, which he joined in 2015. His research program, which has been recognized by a number of awards including the 2019 Cottrell Scholar Award and the 2022 Harry Gray Award for Creative Work in Inorganic Chemistry by a Young Investigator, is broadly directed toward the development of coordination chemistry for biomedical applications.

## ACKNOWLEDGMENTS

We acknowledge financial support from the National Institutes of Biomedical Imaging and Bioengineering of the National Institutes of Health (award numbers R21EB027282 and R01EB029259) and the Research Corporation for Science Advancement through a Cottrell Research Scholar Award to J.J.W.

## REFERENCES


(1) Thiele, N. A.; Brown, V.; Kelly, J. M.; Amor-Coarasa, A.; Jermilova, U.; MacMillan, S. N.; Nikolopoulou, A.; Ponnala, S.; Ramogida, C. F.; Robertson, A. K. H.; Rodríguez-Rodríguez, C.; Schaffer, P.; Williams, C., Jr.; Babich, J. W.; Radchenko, V.; Wilson, J. J. An Eighteen-Membered Macrocyclic Ligand for Actinium-225 Targeted Alpha Therapy. *Angew. Chem., Int. Ed.* **2017**, *56*, 14712−14717.

(2) Hu, A.; MacMillan, S. N.; Wilson, J. J. Macrocyclic Ligands with an Unprecedented Size-Selectivity Pattern for the Lanthanide Ions. *J. Am. Chem. Soc.* **2020**, *142*, 13500−13506.

(3) Abou, D. S.; Thiele, N. A.; Gutsche, N. T.; Villmer, A.; Zhang, H.; Woods, J. J.; Baidoo, K. E.; Escorcia, F. E.; Wilson, J. J.; Thorek, D. L. J. Towards the Stable Chelation of Radium for Biomedical Applications with an 18-Membered Macrocyclic Ligand. *Chem. Sci.* **2021**, *12*, 3733−3742.

(4) Hu, A.; Aluicio-Sarduy, E.; Brown, V.; MacMillan, S. N.; Becker, K. V.; Barnhart, T. E.; Radchenko, V.; Ramogida, C. F.; Engle, J. W.; Wilson, J. J. Py-Macrodipa: A Janus Chelator Capable of Binding Medicinally Relevant Rare-Earth Radiometals of Disparate Sizes. *J. Am. Chem. Soc.* **2021**, *143*, 10429−10440.

(5) *Radiopharmaceutical Chemistry*; Lewis, J. S., Windhorst, A. D., Zeglis, B. M., Eds.; Springer Nature Switzerland AG: Cham, Switzerland, 2019.

(6) Sgouros, G.; Bodei, L.; McDevitt, M. R.; Nedrow, J. R. Radiopharmaceutical Therapy in Cancer: Clinical Advances and Challenges. *Nat. Rev. Drug Discovery* **2020**, *19*, 589−608.

(7) Dondi, M.; Kashyap, R.; Paez, D.; Pascual, T.; Zaknun, J.; Mut Bastos, F.; Pynda, Y. Trends in Nuclear Medicine in Developing Countries. *J. Nucl. Med.* **2011**, *52*, 16S−23S.

(8) Delbeke, D.; Segall, G. M. Status of and Trends in Nuclear Medicine in the United States. *J. Nucl. Med.* **2011**, *52*, 24S−28S.

(9) Blower, P. J. A Nuclear Chocolate Box: the Periodic Table of Nuclear Medicine. *Dalton Trans.* **2015**, *44*, 4819−4844.

(10) Cutler, C. S.; Hennkens, H. M.; Sisay, N.; Huclier-Markai, S.; Jurisson, S. S. Radiometals for Combined Imaging and Therapy. *Chem. Rev.* **2013**, *113*, 858−883.

(11) Boros, E.; Packard, A. B. Radioactive Transition Metals for Imaging and Therapy. *Chem. Rev.* **2019**, *119*, 870−901.

(12) Kostelnik, T. I.; Orvig, C. Radioactive Main Group and Rare Earth Metals for Imaging and Therapy. *Chem. Rev.* **2019**, *119*, 902−956.

(13) Aluicio-Sarduy, E.; Barnhart, T. E.; Weichert, J.; Hernandez, R.; Engle, J. W. Cyclotron-Produced $^{132}La$ as a PET Imaging Surrogate for Therapeutic $^{225}Ac$. *J. Nucl. Med.* **2021**, *62*, 1012−1015.

(14) Bailey, T. A.; Mocko, V.; Shield, K. M.; An, D. D.; Akin, A. C.; Birnbaum, E. R.; Brugh, M.; Cooley, J. C.; Engle, J. W.; Fassbender, M. E.; Gauny, S. S.; Lakes, A. L.; Nortier, F. M.; O'Brien, E. M.; Thiemann, S. L.; White, F. D.; Vermeulen, C.; Kozimor, S. A.; Abergel, R. J. Developing the $^{134}Ce$ and $^{134}La$ Pair as Companion Positron Emission Tomography Diagnostic Isotopes for $^{225}Ac$ and $^{227}Th$ Radiotherapeutics. *Nat. Chem.* **2021**, *13*, 284−289.

(15) Fonslet, J.; Lee, B. Q.; Tran, T. A.; Siragusa, M.; Jensen, M.; Kibédi, T.; Stuchbery, A. E.; Severin, G. W. $^{135}La$ as an Auger-Electron Emitter for Targeted Internal Radiotherapy. *Phys. Med. Biol.* **2018**, *63*, 015026.

(16) Geerlings, M. W.; Kaspersen, F. M.; Apostolidis, C.; van der Hout, R. The Feasibility of $^{225}Ac$ as a Source of $\alpha$-Particles in Radioimmunotherapy. *Nucl. Med. Commun.* **1993**, *14*, 121−125.

(17) Hassfjell, S.; Brechbiel, M. W. The Development of the $\alpha$-Particle Emitting Radionuclides $^{212}Bi$ and $^{213}Bi$, and Their Decay Chain Related Radionuclides, for Therapeutic Applications. *Chem. Rev.* **2001**, *101*, 2019−2036.

(18) Reissig, F.; Kopka, K.; Mamat, C. The Impact of Barium Isotopes in Radiopharmacy and Nuclear Medicine − From Past to Presence. *Nucl. Med. Biol.* **2021**, *98*, 59−68.

(19) Marques, I. A.; Neves, A. R.; Abrantes, A. M.; Pires, A. S.; Tavares-da-Silva, E.; Figueiredo, A.; Botelho, M. F. Targeted Alpha

Therapy Using Radium-223: From Physics to Biological Effects. *Cancer Treat. Rev.* **2018**, *68*, 47−54.
(20) Yong, K.; Brechbiel, M. Application of $^{212}$Pb for Targeted α-particle Therapy (TAT): Pre-clinical and Mechanistic Understanding through to Clinical Translation. *AIMS Med. Sci.* **2015**, *2*, 228−245.
(21) Frantellizzi, V.; Cosma, L.; Brunotti, G.; Pani, A.; Spanu, A.; Nuvoli, S.; De Cristofaro, F.; Civitelli, L.; De Vincentis, G. Targeted Alpha Therapy with Thorium-227. *Cancer Biother. Radiopharm.* **2020**, *35*, 437−445.
(22) Morgenstern, A.; Lebeda, O.; Stursa, J.; Bruchertseifer, F.; Capote, R.; McGinley, J.; Rasmussen, G.; Sin, M.; Zielinska, B.; Apostolidis, C. Production of $^{230}$U/$^{226}$Th for Targeted Alpha Therapy via Proton Irradiation of $^{231}$Pa. *Anal. Chem.* **2008**, *80*, 8763−8770.
(23) Price, E. W.; Orvig, C. Matching Chelators to Radiometals for Radiopharmaceuticals. *Chem. Soc. Rev.* **2014**, *43*, 260−290.
(24) Martell, A. E.; Hancock, R. D. *Metal Complexes in Aqueous Solutions*; Plenum Press: New York, 1996.
(25) Stasiuk, G. J.; Long, N. J. The Ubiquitous DOTA and its Derivatives: the Impact of 1,4,7,10-Tetraazacyclododecane-1,4,7,10-tetraacetic Acid on Biomedical Imaging. *Chem. Commun.* **2013**, *49*, 2732−2746.
(26) Jackson, J. A.; Hungnes, I. N.; Ma, M. T.; Rivas, C. Bioconjugates of Chelators with Peptides and Proteins in Nuclear Medicine: Historical Importance, Current Innovations, and Future Challenges. *Bioconjugate Chem.* **2020**, *31*, 483−491.
(27) Cotton, S. A. Scandium, Yttrium & the Lanthanides: Inorganic & Coordination Chemistry. *Encyclopedia of Inorganic Chemistry*; John Wiley & Sons, Ltd.: Chichester, U.K., 2006.
(28) Shannon, R. D. Revised Effective Ionic Radii and Systematic Studies of Interatomic Distances in Halides and Chalcogenides. *Acta Crystallogr., Sect. A: Found. Adv.* **1976**, *32*, 751−767.
(29) Cheisson, T.; Schelter, E. J. Rare Earth Elements: Mendeleev's Bane, Modern Marvels. *Science* **2019**, *363*, 489−493.
(30) Bünzli, J.-C. G. Lanthanide Luminescence for Biomedical Analyses and Imaging. *Chem. Rev.* **2010**, *110*, 2729−2755.
(31) Wahsner, J.; Gale, E. M.; Rodríguez-Rodríguez, A.; Caravan, P. Chemistry of MRI Contrast Agents: Current Challenges and New Frontiers. *Chem. Rev.* **2019**, *119*, 957−1057.
(32) Piguet, C.; Bünzli, J.-C. G. Mono- and Polymetallic Lanthanide-Containing Functional Assemblies: A Field between Tradition and Novelty. *Chem. Soc. Rev.* **1999**, *28*, 347−358.
(33) Martell, A. E.; Smith, R. M. *Critical Stability Constants*; Plenum Press: New York, 1974; Vol. *1*.
(34) Cacheris, W. P.; Nickle, S. K.; Sherry, A. D. Thermodynamic study of Lanthanide Complexes of 1,4,7-Triazacyclononane-*N*,*N*′,*N*″-triacetic Acid and 1,4,7,10-Tetraazacyclododecane-*N*,*N*′,*N*″,*N*‴-tetra-acetic Acid. *Inorg. Chem.* **1987**, *26*, 958−960.
(35) Moeller, T.; Thompson, L. C. Observations on the Rare Earths—LXXV: The Stabilities of Diethylenetriaminepentaacetic Acid Chelates. *J. Inorg. Nucl. Chem.* **1962**, *24*, 499−510.
(36) Grimes, T. S.; Nash, K. L. Acid Dissociation Constants and Rare Earth Stability Constants for DTPA. *J. Solution Chem.* **2014**, *43*, 298−313.
(37) Chang, C. A.; Rowland, M. E. Metal Complex Formation with 1,10-Diaza-4,7,13,16-tetraoxacyclooctadecane-*N*,*N*′-diacetic Acid. An Approach to Potential Lanthanide Ion Selective Reagents. *Inorg. Chem.* **1983**, *22*, 3866−3869.
(38) Roca-Sabio, A.; Mato-Iglesias, M.; Esteban-Gómez, D.; Tóth, É.; de Blas, A.; Platas-Iglesias, C.; Rodríguez-Blas, T. Macrocyclic Receptor Exhibiting Unprecedented Selectivity for Light Lanthanides. *J. Am. Chem. Soc.* **2009**, *131*, 3331−3341.
(39) Thiele, N. A.; Fiszbein, D. J.; Woods, J. J.; Wilson, J. J. Tuning the Separation of Light Lanthanides Using a Reverse-Size Selective Aqueous Complexant. *Inorg. Chem.* **2020**, *59*, 16522−16530.
(40) Brücher, E.; Győri, B.; Emri, J.; Solymosi, P.; Sztanyik, L. B.; Varga, L. 1,10-Diaza-4,7,13,16-tetraoxacyclooctadecane-1,10-bis-(malonate), a Ligand with High $Sr^{2+}/Ca^{2+}$ and $Pb^{2+}/Zn^{2+}$ Selectivities in Aqueous Solution. *J. Chem. Soc., Chem. Commun.* **1993**, 574−575.
(41) Thiele, N. A.; Woods, J. J.; Wilson, J. J. Implementing f-Block Metal Ions in Medicine: Tuning the Size Selectivity of Expanded Macrocycles. *Inorg. Chem.* **2019**, *58*, 10483−10500.
(42) Regueiro-Figueroa, M.; Esteban-Gómez, D.; de Blas, A.; Rodríguez-Blas, T.; Platas-Iglesias, C. Understanding Stability Trends along the Lanthanide Series. *Chem. - Eur. J.* **2014**, *20*, 3974−3981.
(43) Ferreirós-Martínez, R.; Esteban-Gómez, D.; Tóth, É.; de Blas, A.; Platas-Iglesias, C.; Rodríguez-Blas, T. Macrocyclic Receptor Showing Extremely High Sr(II)/Ca(II) and Pb(II)/Ca(II) Selectivities with Potential Application in Chelation Treatment of Metal Intoxication. *Inorg. Chem.* **2011**, *50*, 3772−3784.
(44) Thiele, N. A.; MacMillan, S. N.; Wilson, J. J. Rapid Dissolution of $BaSO_4$ by Macropa, an 18-Membered Macrocycle with High Affinity for $Ba^{2+}$. *J. Am. Chem. Soc.* **2018**, *140*, 17071−17078.
(45) Fiszbein, D. J.; Brown, V.; Thiele, N. A.; Woods, J. J.; Wharton, L.; MacMillan, S. N.; Radchenko, V.; Ramogida, C. F.; Wilson, J. J. Tuning the Kinetic Inertness of $Bi^{3+}$ Complexes: The Impact of Donor Atoms on Diaza-18-Crown-6 Ligands as Chelators for $^{213}$Bi Targeted Alpha Therapy. *Inorg. Chem.* **2021**, *60*, 9199−9211.
(46) McDevitt, M. R.; Ma, D.; Simon, J.; Frank, R. K.; Scheinberg, D. A. Design and Synthesis of $^{225}$Ac Radioimmunopharmaceuticals. *Appl. Radiat. Isot.* **2002**, *57*, 841−847.
(47) Maguire, W. F.; McDevitt, M. R.; Smith-Jones, P. M.; Scheinberg, D. A. Efficient 1-Step Radiolabeling of Monoclonal Antibodies to High Specific Activity with 225 Ac for α-Particle Radioimmunotherapy of Cancer. *J. Nucl. Med.* **2014**, *55*, 1492−1498.
(48) Deblonde, G. J.-P.; Zavarin, M.; Kersting, A. B. The Coordination Properties and Ionic Radius of Actinium: A 120-Year-Old Enigma. *Coord. Chem. Rev.* **2021**, *446*, 214130.
(49) Aluicio-Sarduy, E.; Hernandez, R.; Olson, A. P.; Barnhart, T. E.; Cai, W.; Ellison, P. A.; Engle, J. W. Production and *in vivo* PET/CT Imaging of the Theranostic Pair $^{132/135}$La. *Sci. Rep.* **2019**, *9*, 10658.
(50) Aluicio-Sarduy, E.; Thiele, N. A.; Martin, K. E.; Vaughn, B. A.; Devaraj, J.; Olson, A. P.; Barnhart, T. E.; Wilson, J. J.; Boros, E.; Engle, J. W. Establishing Radiolanthanum Chemistry for Targeted Nuclear Medicine Applications. *Chem. - Eur. J.* **2020**, *26*, 1238−1242.
(51) Kluetz, P. G.; Pierce, W.; Maher, V. E.; Zhang, H.; Tang, S.; Song, P.; Liu, Q.; Haber, M. T.; Leutzinger, E. E.; Al-Hakim, A.; Chen, W.; Palmby, T.; Alebachew, E.; Sridhara, R.; Ibrahim, A.; Justice, R.; Pazdur, R. Radium Ra 223 Dichloride Injection: U.S. Food and Drug Administration Drug Approval Summary. *Clin. Cancer Res.* **2014**, *20*, 9−14.
(52) Reissig, F.; Bauer, D.; Ullrich, M.; Kreller, M.; Pietzsch, J.; Mamat, C.; Kopka, K.; Pietzsch, H.-J.; Walther, M. Recent Insights in Barium-131 as a Diagnostic Match for Radium-223: Cyclotron Production, Separation, Radiolabeling, and Imaging. *Pharmaceuticals* **2020**, *13*, 272.
(53) Lewington, V. J. Bone-Seeking Radionuclides for Therapy. *J. Nucl. Med.* **2005**, *46*, 38S−47S.
(54) Shimoni-Livny, L.; Glusker, J. P.; Bock, C. W. Lone Pair Functionality in Divalent Lead Compounds. *Inorg. Chem.* **1998**, *37*, 1853−1867.
(55) Pujales-Paradela, R.; Rodríguez-Rodríguez, A.; Gayoso-Padula, A.; Brandariz, I.; Valencia, L.; Esteban-Gómez, D.; Platas-Iglesias, C. On the Consequences of the Stereochemical Activity of the Bi(iii) $6s^2$ Lone Pair in Cyclen-Based Complexes. The [Bi(DO3A)] Case. *Dalton Trans.* **2018**, *47*, 13830−13842.
(56) Baba, K.; Nagata, K.; Yajima, T.; Yoshimura, T. Synthesis, Structures, and Equilibrium Reactions of La(III) and Ba(II) Complexes with Pyridine Phosphonate Pendant Arms on a Diaza-18-crown-6 Ether. *Bull. Chem. Soc. Jpn.* **2022**, DOI: 10.1246/bcsj.20210414.
(57) Panchenko, P. A.; Zubenko, A. D.; Chernikova, E. Y.; Fedorov, Y. V.; Pashanova, A. V.; Karnoukhova, V. A.; Fedyanin, I. V.; Fedorova, O. A. Synthesis, Structure and Metal Ion Coordination of Novel Benzodiazamacrocyclic Ligands Bearing Pyridyl and Picolinate Pendant Side-Arms. *New J. Chem.* **2019**, *43*, 15072−15086.


https://doi.org/10.1021/acs.accounts.2c00003
*Acc. Chem. Res.* 2022, 55, 904−915

(58) Zeglis, B. M.; Lewis, J. S. A Practical Guide to the Construction of Radiometallated Bioconjugates for Positron Emission Tomography. *Dalton Trans.* **2011**, *40*, 6168−6195.
(59) Lattuada, L.; Barge, A.; Cravotto, G.; Giovenzana, G. B.; Tei, L. The Synthesis and Application of Polyamino Polycarboxylic Bifunctional Chelating Agents. *Chem. Soc. Rev.* **2011**, *40*, 3019−3049.
(60) Kwon, H.; Son, S.-H.; Byun, Y. Prostate-Specific Membrane Antigen (PSMA)-Targeted Radionuclide Probes for Imaging and Therapy of Prostate Cancer. *Asian J. Org. Chem.* **2019**, *8*, 1588−1600.
(61) Dumelin, C. E.; Trüssel, S.; Buller, F.; Trachsel, E.; Bootz, F.; Zhang, Y.; Mannocci, L.; Beck, S. C.; Drumea-Mirancea, M.; Seeliger, M. W.; Baltes, C.; Müggler, T.; Kranz, F.; Rudin, M.; Melkko, S.; Scheuermann, J.; Neri, D. A Portable Albumin Binder from a DNA-Encoded Chemical Library. *Angew. Chem., Int. Ed.* **2008**, *47*, 3196−3201.
(62) Kelly, J. M.; Amor-Coarasa, A.; Ponnala, S.; Nikolopoulou, A.; Williams, C.; Thiele, N. A.; Schlyer, D.; Wilson, J. J.; DiMagno, S. G.; Babich, J. W. A Single Dose of $^{225}$Ac-RPS-074 Induces a Complete Tumor Response in an LNCaP Xenograft Model. *J. Nucl. Med.* **2019**, *60*, 649−655.
(63) Bell, M. M.; Gutsche, N. T.; King, A. P.; Baidoo, K. E.; Kelada, O. J.; Choyke, P. L.; Escorcia, F. E. Glypican-3-Targeted Alpha Particle Therapy for Hepatocellular Carcinoma. *Molecules* **2021**, *26*, 4.
(64) Ishiguro, T.; Sugimoto, M.; Kinoshita, Y.; Miyazaki, Y.; Nakano, K.; Tsunoda, H.; Sugo, I.; Ohizumi, I.; Aburatani, H.; Hamakubo, T.; Kodama, T.; Tsuchiya, M.; Yamada-Okabe, H. Anti−Glypican 3 Antibody as a Potential Antitumor Agent for Human Liver Cancer. *Cancer Res.* **2008**, *68*, 9832−9838.
(65) Reissig, F.; Bauer, D.; Zarschler, K.; Novy, Z.; Bendova, K.; Ludik, M.-C.; Kopka, K.; Pietzsch, H.-J.; Petrik, M.; Mamat, C. Towards Targeted Alpha Therapy with Actinium-225: Chelators for Mild Condition Radiolabeling and Targeting PSMA—A Proof of Concept Study. *Cancers* **2021**, *13*, 1974.
(66) Haldón, E.; Nicasio, M. C.; Pérez, P. J. Copper-Catalysed Azide−Alkyne Cycloadditions (CuAAC): An Update. *Org. Biomol. Chem.* **2015**, *13*, 9528−9550.
(67) Hu, A.; Wilson, J. J. Unpublished result.
(68) Li, L.; Jaraquemada-Peláez, M.; de, G.; Kuo, H.-T.; Merkens, H.; Choudhary, N.; Gitschtaler, K.; Jermilova, U.; Colpo, N.; Uribe-Munoz, C.; Radchenko, V.; Schaffer, P.; Lin, K.-S.; Bénard, F.; Orvig, C. Functionally Versatile and Highly Stable Chelator for $^{111}$In and $^{177}$Lu: Proof-of-Principle Prostate-Specific Membrane Antigen Targeting. *Bioconjugate Chem.* **2019**, *30*, 1539−1553.
(69) Hu, A.; Keresztes, I.; MacMillan, S. N.; Yang, Y.; Ding, E.; Zipfel, W. R.; DiStasio, R. A., Jr.; Babich, J. W.; Wilson, J. J. Oxyaapa: A Picolinate-Based Ligand with Five Oxygen Donors that Strongly Chelates Lanthanides. *Inorg. Chem.* **2020**, *59*, 5116−5132.
(70) Hu, A.; Brown, V.; MacMillan, S. N.; Radchenko, V.; Yang, H.; Wharton, L.; Ramogida, C. F.; Wilson, J. J. Chelating the Alpha Therapy Radionuclides $^{225}Ac^{3+}$ and $^{213}Bi^{3+}$ with 18-Membered Macrocyclic Ligands Macrodipa and Py-Macrodipa. *Inorg. Chem.* **2022**, *61*, 801−806.





https://doi.org/10.1021/acs.accounts.2c00003
*Acc. Chem. Res.* 2022, 55, 904−915